SSRG International Journal of Electrical and Electronics Engineering
ISSN: 2348-8379/ https://doi.org/10.14445/23488379/IJEEE-V10I7P119

Volume 10 Issue 7, 211-220, July 2023

Original Article

Impact of Fuzzy PID and PSO-PID Controllers on the Load Frequency Control of Interconnected Microgrids

Ranjit Singh[1], L. Ramesh[2]

[1,2]*EEE, Dr. M.G.R Educational and Research Institute, Tamil Nadu, India.*

[1]*Corresponding Author : rsa.ranjit@gmail.com*

Received: 29 April 2023 Revised: 27 June 2023 Accepted: 14 July 2023 Published: 31 July 2023

Abstract *- Microgrid technology is an alternative to the central grid for the electrification of the whole world and is termed an energy grid that can disconnect itself from the traditional grid and run independently. The grid acts as a bridge to connect residential buildings, houses, and small loads to the primary power sources. This type of interconnection has a demerit: when a fault in any part of the grid must be replaced, the rest of the system connected to it is also affected tremendously. Therefore, a microgrid acts as a primary option in this case. This paper aims to minimize the frequency deviations, which are the primary cause of power failures and disrupted electrical power flow. The load frequency control strategy has been employed to balance the generation and load. The model is simulated in MATLAB fuzzy PID Controller and PSO-PID Controller to minimize 2014b and the frequency deviations. The PSO Algorithm codes are designed on MATLAB function file, which helped to calibrate the gains of PID Controller in both the microgrids. The primary outcome of this article is the study of frequency oscillations and area control error, along with the impact of both controllers on the system. The necessary graphs indicate the capability of the PSO-PID controller when collated with a fuzzy PID Controller. Also, the robustness of the controllers is obtained by the dynamic load changes in each microgrid. The PSO-PID controller is quick and gives more accurate results in minimizing overshoot, error reduction, and rise time.*

Keywords *- Area Control Error, Distributed energy sources, Frequency deviations, PSO algorithm, UNSDG.*

1. Introduction

With the demand for electricity increasing daily, it has become a global challenge to produce considerable electrical energy considering the availability of resources like coal, natural gas, petroleum, and nuclear energy. However, these resources are non-renewable and are used quickly daily; thus, their availability will be a significant problem in the coming years. There is another category of resources from which electricity can be produced on a vast scale, creating no environmental pollution. These resources are renewable sources of energy and are categorized into solar, wind, hydro, tidal, geothermal and biomass [1], [2], [3]. Renewable energy resources have many merits, including their availability, i.e., they never run out. Apart from this, these resources cause less pollution and have easy maintenance.

Microgrids are a group of resources that uses renewable sources to produce electrical energy and can fulfil the excessive demand for electrical power wherever required [4]. Microgrids can be classified into three types which are remote, grid-connected and networked. Remote Microgrids are physically isolated from the primary grid and work in island style frequently because of the unavailability of proper support for the transmission and distribution of electrical power; for these remotely based microgrids, wind and solar are the best alternatives to other energy sources that provide economical Distributed Energy Resource solutions for the microgrid engineer. Battery energy storage systems are used instead of traditional generators for providing power backup in remote microgrids [5], [6], [7], [8]. A microgrid connected to the primary grid can benefit it by addressing issues like power quality, accuracy, and voltage problems associated with the grid. Battery energy storage systems have significantly helped provide emergency backup power for the microgrids operating in grid-connected and island modes. Microgrids are essential in serving educational institutions, parks, and commercial buildings by providing power in case of emergencies or power failures. Interconnected Microgrids, also called interlocked microgrids, consist of various DERs [9], [10]. A regulatory control system manages and optimizes the networked microgrids for proper operation and coordination with each grid-connected source.

When there is an interconnection between the two microgrids shown in Figure 1, transmitting power to the connected grid becomes straightforward, which requires more energy during increased demand [11], [12].

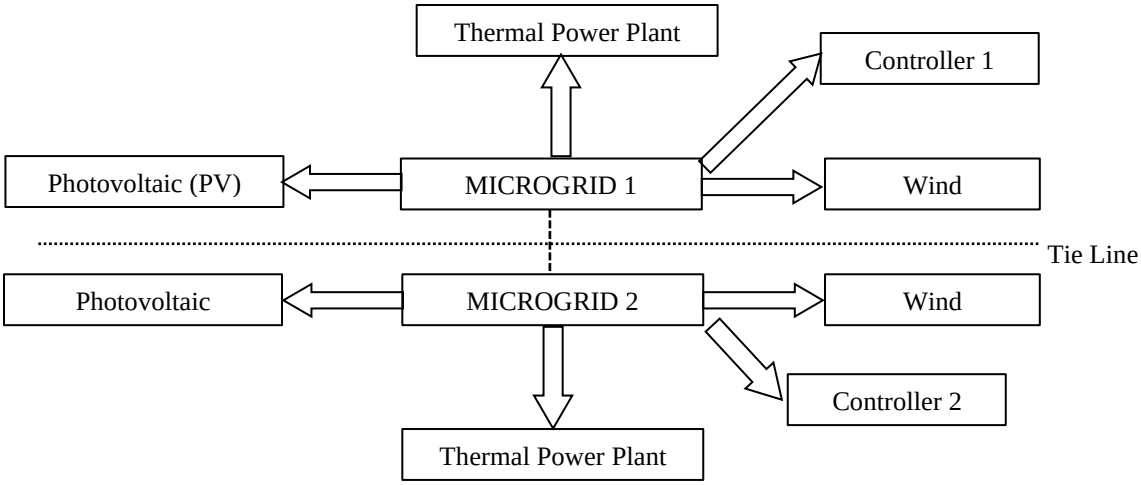

Fig. 1 Model of interconnected microgrids

However, there are important parameters that have to be balanced and kept in a nominal range. These parameters are frequency deviations caused by the imbalance between the generation and demand in a microgrid along with ACE. The transmission lines break due to the over or under frequency which becomes a significant cause of grid failure [13], [14]. Using controllers and different optimization algorithms can solve this problem. According to recent research, around 236 million people experience energy shortages. Thus the government of India has taken the initiative to set up at least 12,000 micro or mini-grids with more than 500 MW of generation capacity[15].

Load frequency stability is always considered a crucial factor in maintaining the stability of power systems [16]. For a microgrid system, if the difference between generation and demand continues to occur in the system, then a quick and reliable frequency controller is required that can quickly reduce the error in a quick time. In this paper, the Simulink model is simulated using a PID controller and the controller is tuned with the system to get the gains of P, I, D. Also, the simulation is carried by a fuzzy PID Controller and necessary graphs are obtained to see the performance of the controller in controlling and minimizing the system frequency.

This paper has the following sections apart from the Introduction: Section 2 focuses on the methodology and design of the Controllers used in the circuit. Section 3 explains the Simulink Model of Interconnected Microgrids. System Equations is formulated in Section 4. Section 5 focuses on the Results and Graphs. The Last Section highlights the conclusion of the work.

2. Research Methodology and Design of Controllers

This section explains the methodology and design of different controllers in simulating the system model. Also, the Load Frequency Control (LFC) control strategy employed in the simulation is discussed in detail.

2.1. Load Frequency Control (LFC)

The LFC loop regulates the actual output power and the corresponding frequency of the generator power output. The primary LFC controls the speed of the Turbine, and the primary LFC controls the Turbine's power through the speed governor [18], [29]. The sensing ability of the primary LFC loop is faster than the secondary LFC loop, senses the electrical frequency which comes out of the generator and maintains the proper flow of power, including power interchange with the interconnected areas in the network. The secondary LFC loop is slower in response and very slow to respond to the fast frequency and load changes. Usually, the primary LFC loop operates in the order of seconds, while it takes a few minutes for the secondary LFC loop to operate. Figure 2 shows the LFC loop's primary function, which reduces the deviations and errors to zero and thus restoring the balance between generation and load by controlling speed [19].

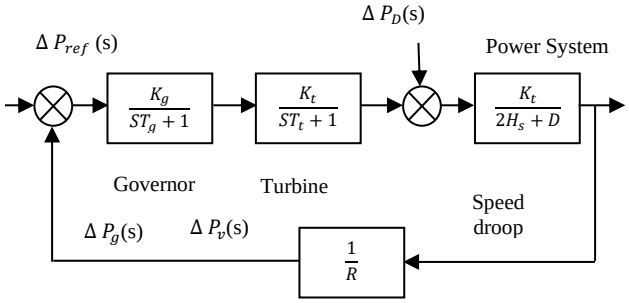

Fig. 2 Load frequency control loop in a system

This control mechanism is applied to the Simulink model to bring the frequency deviation to the null position and thus preserve the system's stability.

2.2. A Proportional-Integral-Derivative (PID) Controller

The difference between a quantity/ value and a final set point is an error value controlled by the PID controller [20]. The gains of parameters are tuned to upgrade the system output in terms of error reduction time. Figure 3 shows the PID Controller representation where proportional gain, integral gain, and change in error value and time [30].

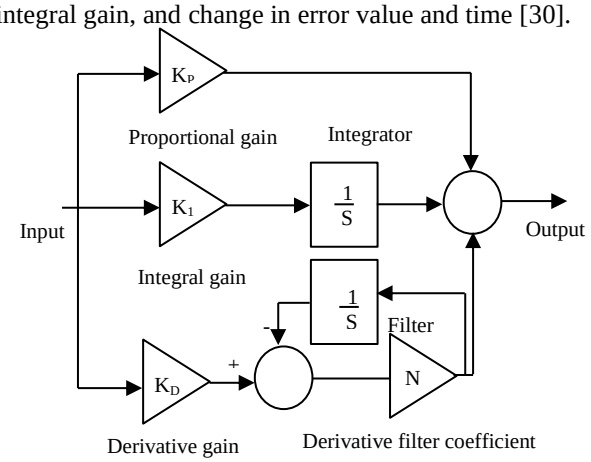

Fig. 3 Model of a PID Controller

The controller must sense the changes in frequency and load in a quick time [22]. The PID Controller controls the frequency, and its performance and the necessary graphs are observed [23]. Nowadays, intelligent controllers have replaced the standard controllers to obtain the system response faster and more accurately.

One of them is fuzzy PID which is discussed below:

$$y(t) = K_p[e(t) + T_d \frac{d(e)}{d(t)} + \frac{1}{T_i}\int_0^t e(t)d(t)] \quad (1)$$

$$y(t) = K_p[e(t) + K_d \frac{d(e)}{d(t)} + K_i \int_0^t e(t)d(t) \quad (2)$$

$$K_i = \frac{K_p}{T_i} \quad (3)$$

$$K_d = K_p.T_d \quad (4)$$

In Equation (1), the output signal y(t) is obtained after the proportional, Integral and derivative controllers tune the error. The main objective is to minimize the error and keep it under a nominal range. The ki and kd values are shown in Equations (2) and (3), respectively.

2.3. Fuzzy Tuned PID Controller

Fuzzy controllers are considered more advantageous than classical controllers because of the simple control mechanism, which is low-cost and can tune without the model parameters. Figure 4 shows a fuzzy PID Controller subsystem model where the error signal is passed to the Proportional, Derivative and Integral and fed to the Fuzzy system where the values are tuned.

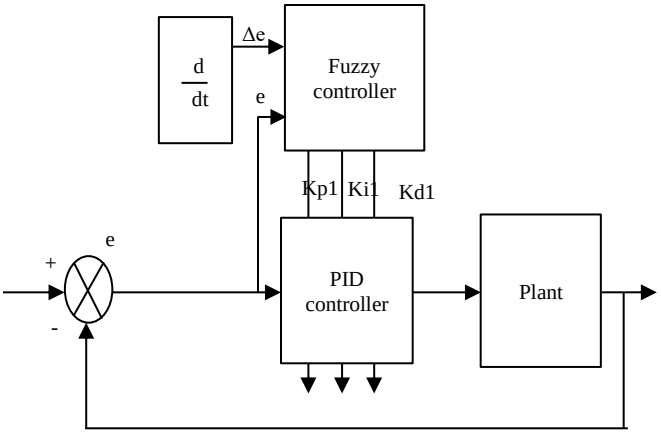

Fig. 4 Subsystem of a fuzzy-tuned PID Controller

Figure 5 shows the four main blocks of the fuzzy logic controller. The crisp data is converted to linguistic format using a fuzzification block [24]. The Decision-Making Unit consists of a rule base that provides linguistic rules and an inference engine that provides data that helps finalize the required format.

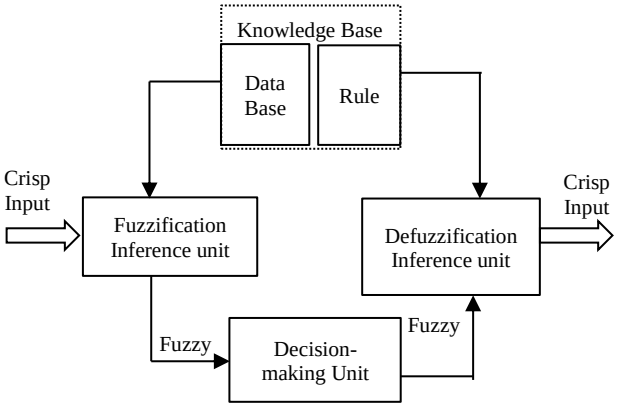

Fig. 5 Main blocks of fuzzy PID controller

$$e(t) = E_{ref} - E_g \quad (5)$$

$$de(t) = e(t) - e(t-1) \quad (6)$$

The defuzzification unit takes the output of the DMU block as its input, and here the fuzzy back is converted to a crisp signal. The DMU uses the rules of "IF-THEN-ELSE". The inference block takes the error and its derivative as input and tunes the controller's gains.

2.4. PSO-PID Controller

PSO-PID Controller helps minimise the system frequency deviations as Particle Swarm Optimization (PSO) Algorithm tunes the PID controller gains. The codes of the PSO Algorithm are made and run as MATLAB Code files. The results obtained after running the codes give the numerical results of the PID Controller gains, and these values, when put in the system, give an auspicious result. The primary

important outcome of the algorithm is that the gains of the PID controller are tuned by considering the swarm of different random variables.

(PSO) is a technique that aims to improve a candidate solution based on iterations, optimizing it based on a specified quality measure [31]. It tackles problems by utilizing a group of candidates as particles and manipulating their positions and velocities within the search environment using formulas [26]. Each particle is determined by the local best-known position near it while deviating towards the global best-known positions, which are upgraded as other particles discover superior solutions. This collaborative movement is designed to steer the swarm towards optimal solutions. Initially, PSO was developed by Kennedy, Eberhart, and Shi to simulate social behaviour inspired by the collective motion of birds in a group or fish in an organization [27].

Figure 6 shows the PSO Algorithm's flowchart, which serves as the base for writing the codes in MATLAB.

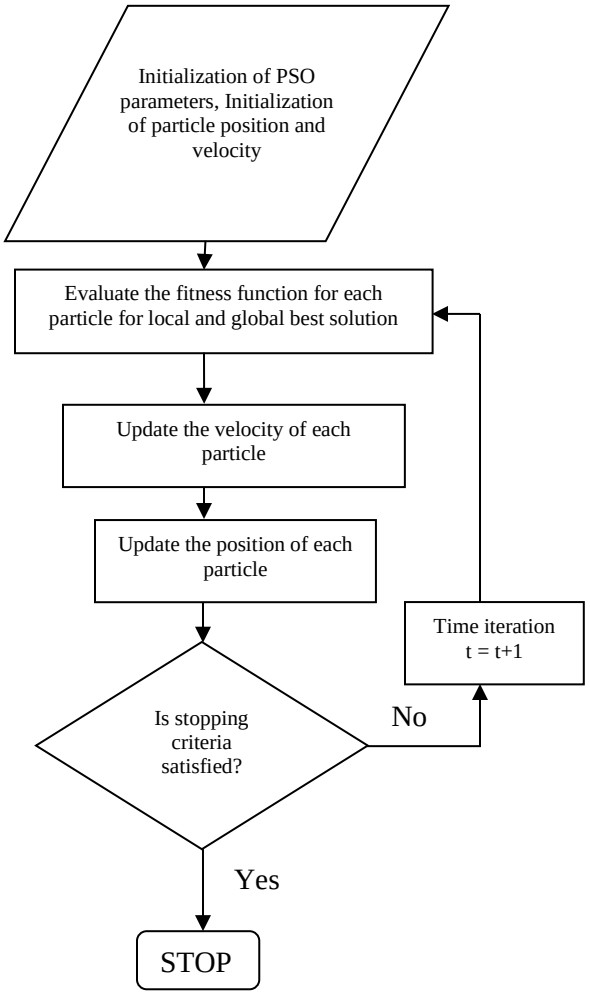

Fig. 6 Flowchart of a PSO- PID controller

Over time, the algorithm exhibited effective optimization capabilities. Kennedy and Eberhart's book delves into the analytical features of PSO and swarm observation, while Poli has conducted an extensive survey on various applications of PSO [28].

An optimization problem aims at finding a variable shown by a vector X = [x1, x2, x3, ..., xn] that reduces a function f(X) based on the optimization formulation. For instance, in determining a landing point for a flock, the variables could represent latitude and longitude. The function f(X), also called the fitness function or objective function, evaluates the quality of a position X, reflecting how favourable a bird perceives a certain landing point after discovering it. This evaluation typically considers various survival criteria.

In a swarm consisting of P particles, each particle I has a position vector and a velocity vector. Both these vectors are updated in the following equations:

$$V_{ij}^{t+1} = wV_{ij}^{t} + c_1 r_1^t \left(pbest_{ij} - X_{ij}^{t}\right) + c_2\, r_2^t \left(gbest_j - X_{ij}^{t}\right) \tag{7}$$

$$X_{ij}^{t+1} = X_{ij}^{t} + X_{ij}^{t+1} \tag{8}$$

Figure 7 shows the velocity and position updates from many variables. The main aim is to find the best value to fit the desired system.

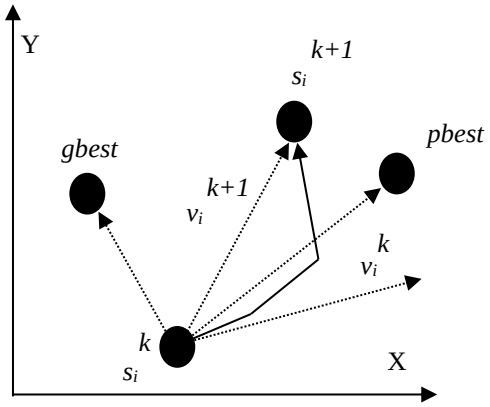

Fig. 7 Velocity and position updates

3. Simulink Model of Interconnected Microgrids

Figure 8 depicts the IEEE-based (LFC) of two Interconnected Microgrids. Microgrids 1 and 2 comprise a thermal power plant, photovoltaic (PV) system, and wind energy generation. This section explains the modelling of the thermal power plant, Battery storage, photovoltaic (PV) and wind turbine as a transfer function with values assigned to the gains and constants of every transfer function.

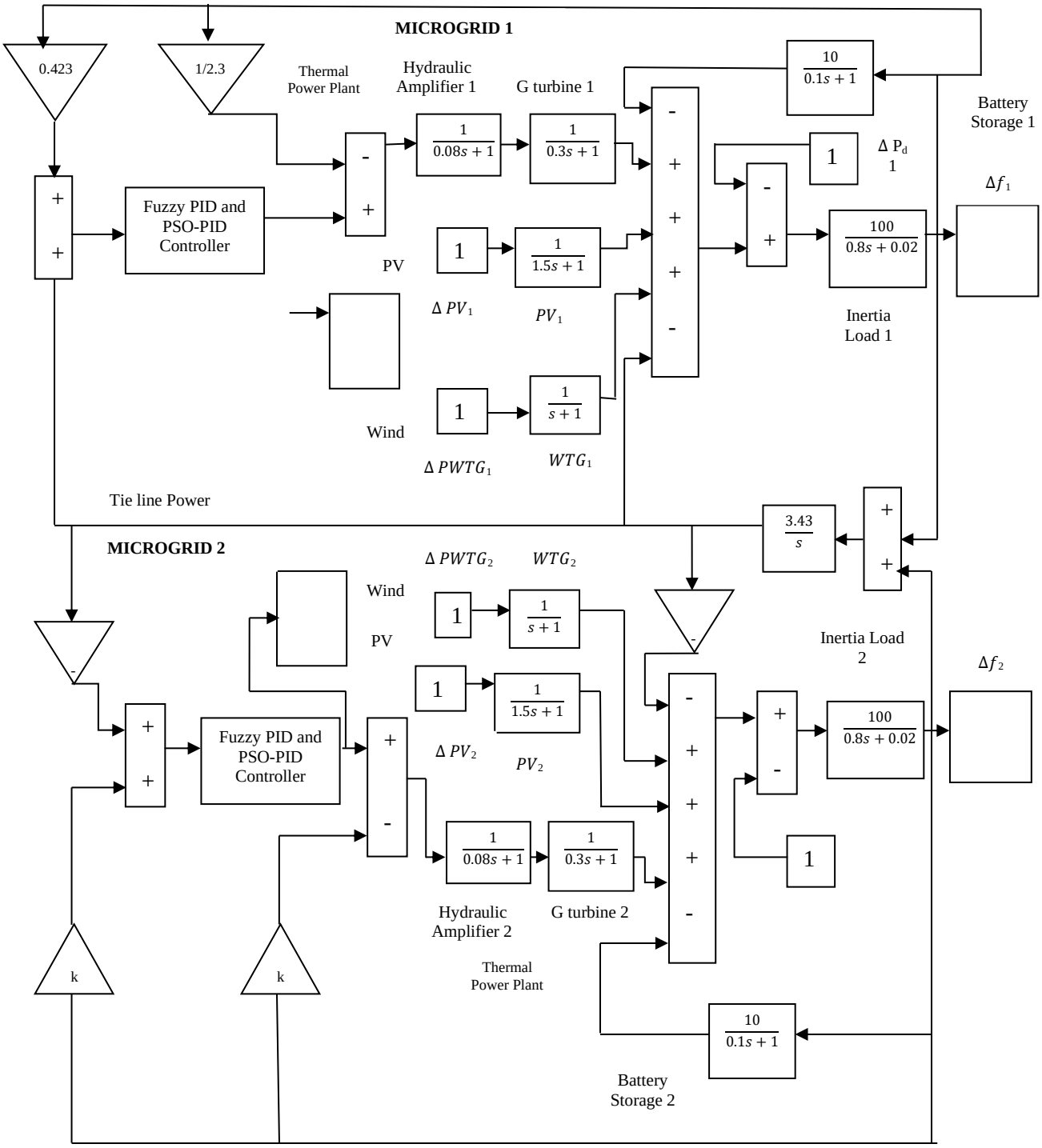

Fig. 8 IEEE-based LFC of interconnected microgrids

3.1. Modelling of Generator (Wind Turbine)

The wind speed is one of the significant factors on which the generator's output depends.

The mechanical power output of the wind turbine is provided below:

$$P_{WT} = 1/2\ \rho A_r C_p V_W^3 \quad (9)$$

where,

ρ= Density of Air (kg/m^3)

A_r= Area Swept by the blade (m^2)

C_p= Power coefficient

Vw= Wind velocity (m/s)

The transfer function can be formulated as follows:

$$G_{WTG}(s) = \frac{\Delta P_{WTG}}{\Delta P_{WT}} = \frac{K_{WTG}}{1+sT_{WTG}} \quad (10)$$

where,

K_{WTG}= Turbine generator gain and

T_{WTG} =Turbine Generator time constant

3.2. Modelling of Photovoltaic (PV) System

The desired voltage and current values are provided by the solar photovoltaic (PV) system.

The output power of the system is given below:

$$P_{pv} = \eta M \phi [1 - 0.005\ (T_{at} + 25)] \quad (11)$$

The transfer function of the Photovoltaic system is given below:

$$G_{pv}(s) = \frac{\Delta P_{pv}}{\Delta \emptyset} = \frac{K_{pv}}{(1+sT_{pv})} \quad (12)$$

3.3. Modelling of Energy Storage System

Energy storage systems play a crucial role in rapidly supplying energy to maintain system stability in hybrid power systems.

$$G_{ESS}(s) = \frac{\Delta P_{ESS}}{\Delta f} = \frac{K_{ESS}}{1+sT_{ESS}} \quad (13)$$

3.4. Modelling of Amplifier and Turbine of Thermal Power Plant

The primary function of a hydraulic amplifier is to regulate the flow of steam and operate the valve.

$$G_{amp} = \frac{K_{amp}}{1+sT_{amp}} \quad (14)$$

Following is the transfer function of the Turbine block given as:

$$\mathrm{G_t} = \frac{\mathrm{K_t}}{1+\mathrm{sT_t}} \quad (15)$$

3.5. Variations in Frequency and Power Fluctuations of the System

The output power must be controlled based on power demand to maintain stable operation. The total generated power of the system (PT) can be calculated by summing up the power generated by all the connected devices and generators, such as wind power (PWTG) and the power of the solar photovoltaic system (PPV).

The values for PWTG and PPV are provided below:

$$P_T = P_{TH} + P_{WTG} + P_{pv} \quad (16)$$

The difference between P_T and P_D is given by

$$P_E = P_T - P_D \quad (17)$$

The frequency variation Δf is given below:

$$\Delta f = \frac{\Delta P_E}{K_{sys}} \quad (18)$$

The transfer function representing the relationship between frequency variation and per-unit power fluctuation is provided below:

$$G_{sys}(s) = \frac{\Delta f}{\Delta P_E} = \frac{1}{K_{sys}(1+sT_{sys})} = \frac{1}{D_m+I_s} \quad (19)$$

4. Results and Discussion

This section explains the graphs from the MATLAB simulation of two interconnected microgrids using a fuzzy PID Controller and PSO-PID Controller. The details and observations for each graph are as follows:

Figure 9- Frequency Deviation in Microgrid 1 (Fuzzy PID Controller)-The graph illustrates the change in frequency in MG1 1 when the fuzzy PID Controller simulates the system model. It is observed that the deviation in frequency is gradually reduced to zero within 13 seconds.

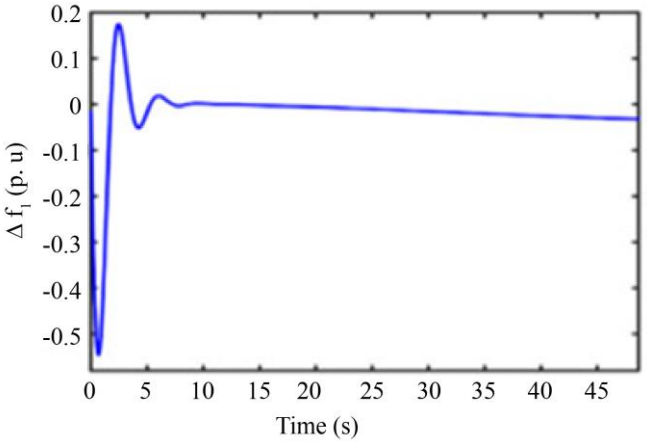

Fig. 9 Frequency deviations in MG 1 using fuzzy PID controller

Figure 10- Frequency Deviation in Microgrid 2 (Fuzzy PID Controller)-This graph represents the change in frequency deviation in MG 2 when the fuzzy PID Controller simulates the system model. It is observed that the deviation in frequency reaches zero within 12 seconds.

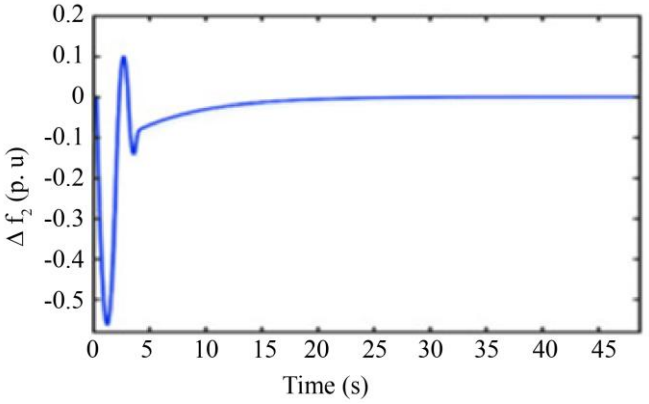

Fig. 10 Frequency deviations in MG 2 using fuzzy PID controller

Figure 11- Frequency Deviation in Microgrid 1 (PSO-PID Controller)-The graph showcases the change in frequency deviation in MG 1 when the PSO-PID Controller simulates the system model. It is observed that the deviation in frequency is significantly reduced to zero within a short time of 2.2 seconds.

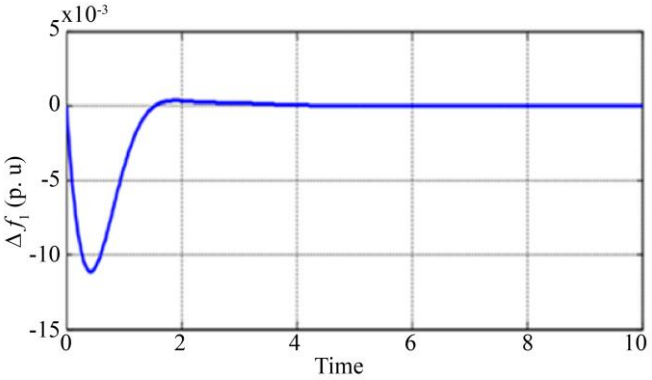

Fig. 11 Frequency deviations in MG 1 using PSO-PID controller

Figure 12- Frequency Deviation in Microgrid 2 (PSO-PID Controller)-This graph demonstrates the change in frequency deviation in MG 2 when the PSO-PID Controller simulates the system model. It is observed that the deviation in frequency is brought to zero in approximately 8 seconds.

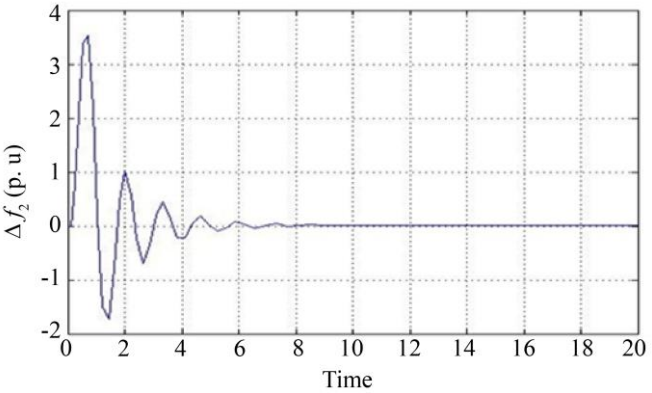

Fig. 12 Frequency deviations in MG 2 using PSO-PID controller

Figure 13 the Area Control Error is shown when the system model is simulated using a fuzzy PID Controller, which takes 18 seconds to tie line power to zero.

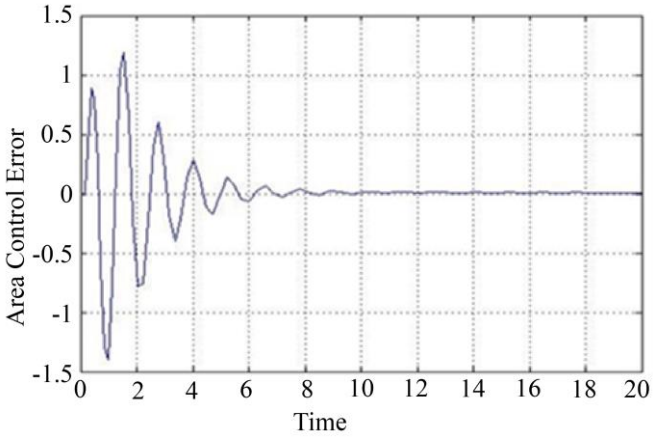

Fig. 13 Area Control Error of the system using fuzzy PID Controller

Figure 14 shows the Area Control Error when the system model is simulated using PSO-PID Controller, where it takes only 9 seconds for the tie line power to come to a null position.

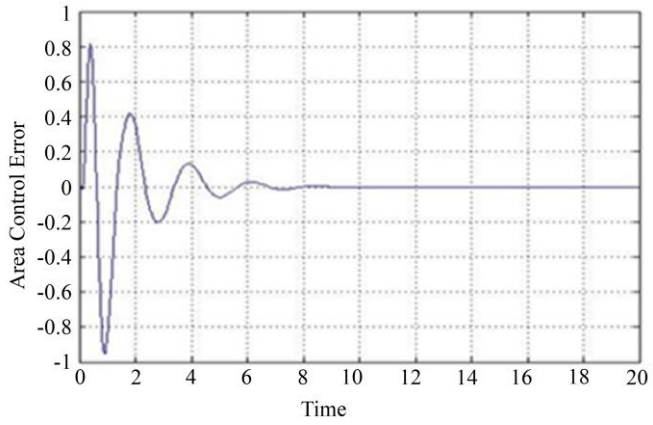

Fig. 14 Area Control Error of the system using PSO-PID controller

These graphs provide insights into the performance and effectiveness of the fuzzy PID Controller and PSO-PID Controller in maintaining frequency and reducing error in the interconnected microgrids.

The observations obtained from the graphs indicate that the PSO-PID Controller has better performance criteria than the fuzzy PID Controller in terms of the time taken to reduce frequency deviations and area control error in the interconnected microgrids.

The PSO-PID Controller shows faster convergence and achieves zero frequency deviation and reduced error in a shorter time. This suggests that the PSO-PID Controller showcases superior performance in maintaining system stability and controlling power fluctuations in the Microgrids.

Equations

The system equations used in the interconnection of the two microgrids are presented as follows:

$$\Delta f(s) = G_P(s)[\Delta P_T(s) - \Delta P_D(s)] \quad (20)$$

$$\Delta f_1 \propto \Delta P_{T1} - \Delta P_{D1} - \Delta P_{12} + P_{T(PV1)} + P_{T(WT1)} + P_{TH1} \quad (21)$$

$$\Delta f_2 \propto \Delta P_{T2} - \Delta P_{D2} - \Delta P_{21} + P_{T(PV2)} + P_{T(WT2)} + P_{TH2} \quad (22)$$

The Area Control Errors (ACEs) for two interconnected areas are presented as follows:

$$ACE_1 = \Delta P_{12} + C_1 \Delta f_1 \quad (23)$$

$$ACE_2 = -\Delta P_{21} + C_2 \Delta f_2 \quad (24)$$

The following equation represents the incremental change in tie-line power:

$$\Delta P_{tie1} = \frac{2\Pi T_{12}}{s} [\Delta f_1(s) - \Delta f_2(s)] \quad (25)$$

Table 1 indicates the performance of the two controllers in terms of the time required to minimize the error in the system.

The values indicated in the table show that the parameters minimized by the two controllers are changes in frequency in MG 1 and MG 2, Tie line power flowing between 2 interconnected microgrids.

Table 1. Responses of fuzzy PID and PSO-PID controllers

Parameters	Fuzzy PID controller (secs)	PSO-PID controller (secs)
Δf_1 in MG 1	13	2.2
Δf_2 in MG 2	12	8
Area Control Error	18	9

5. Conclusion

This paper uses the load frequency control method to investigate the impact of fuzzy- PID controller and PSO - PID controller on interconnected microgrids. The frequency deviations in Microgrid 1 and 2 are reduced in 13 seconds and 12 seconds, respectively, when the system is simulated using a fuzzy PID Controller. In contrast, when controlled by PSO-PID Controller, it is 2.2 seconds for Microgrid 1 and 8 seconds for Microgrid 2. The PSO algorithm tunes the PID controller gains, and the frequency responses in both microgrids are observed. Microgrid 2 has a better frequency response as the whole system is simulated using the algorithm, and the tuned values of K_p, K_i and K_d are put in both microgrids to obtain the frequency response. The results are compared with the responses obtained from the fuzzy PID controller.

The frequency deviations are indeed reduced more rapidly by the PSO-PID Controller compared to the fuzzy PID Controller. Also, the Area Control Errors in both the microgrids are minimized to zero in 18 seconds and 9 seconds using fuzzy PID and PSO-PID Controller, respectively. The main objective of the paper is to contribute to the United Nations Sustainable Development Goal (UNSDG) 7, which focuses on affordable and clean energy. This goal aims to ensure access to affordable, reliable, sustainable, and modern energy for all by the year 2030. By utilizing advanced control techniques like the PSO-PID Controller, the research aims to enhance the stability and efficiency of microgrid systems, thereby contributing to the broader objective of achieving affordable and clean energy for global sustainable development. Also, investing in solar, wind and thermal power helps improve future energy productivity.

This paper is contributing to UNSDG 7 as, in future, microgrids will be the primary source of electricity generation, including distribution. Moreover, the generating plants used in this paper for simulation are all renewable energy sources. Moreover, all the countries in the coming future will rely upon renewable energy and every country will aim to achieve affordable, reliable energy for all the people. The simulation can be implemented in practical applications as it ensures an active electrical power exchange between interconnected microgrids. Further work can be done in this Area of research by increasing the number of microgrids and enabling fast and quick error settling time for frequency minimizations by more sophisticated algorithms.

References

[1] Farshid Shariatzadeh, Nikhil Kumar, and Anurag K. Srivastava, "Optimal Control Algorithms for Reconfiguration of Shipboard Microgrid Distribution System using Intelligent Techniques," *IEEE Transactions on Industry Applications*, vol. 53, no. 1, pp. 474-482, 2017. [CrossRef] [Google Scholar] [Publisher Link]

[2] A. A. Salam, A. Mohamed, and M. A. Hannan, "Technical Challenges on Microgrids," *ARPN Journal of Engineering and Applied Sciences*, vol. 3, no. 6, 2008. [Google Scholar] [Publisher Link]

[3] Deepak Kumar Lal, Ajit Kumar Barisal, and M. Tripathy, "Load Frequency Control of Multi Area Interconnected Microgrid Power System using Grasshopper Optimization Algorithm Optimized Fuzzy PID Controller," *Recent Advances on Engineering, Technology and Computational Sciences*, Allahabad, pp. 1-6, 2018. [CrossRef] [Google Scholar] [Publisher Link]

[4] Mukwanga W. Siti et al., “Optimal Frequency Deviations Control in Microgrid Interconnected Systems,” *IET Renewable Power Generation*, vol. 13, no. 13, pp. 2376-2382, 2019. [CrossRef] [Google Scholar] [Publisher Link]

[5] Lei Xi et al., "A Virtual Generation Ecosystem Control Strategy for Automatic Generation Control of Interconnected Microgrids," *IEEE Access*, vol. 8, pp. 94165-94175, 2020. [CrossRef] [Google Scholar] [Publisher Link]

[6] Pietro Ferraro et al., "Stochastic Frequency Control of Grid-Connected Microgrids," *IEEE Transactions on Power Systems*, vol. 33, no. 5, pp. 5704-5713, 2018. [CrossRef] [Google Scholar] [Publisher Link]

[7] Saroja Kanti Sahoo, and Nudurupati Krishna Kishore, “Battery State-of-Charge-Based Control and Frequency Regulation in the MMG System using Fuzzy Logic,” *IET Generation, Transmission and Distribution*, vol. 14, no. 14, pp. 2698-2709, 2020. [CrossRef] [Google Scholar] [Publisher Link]

[8] Abdul Latif et al., “Illustration of Demand Response Supported Coordinated System Performance Evaluation of YSGA Optimized Dual Stage PIFOD-(1 + PI) Controller Employed with Wind-Tidal-Biodiesel based Independent Two-Area Interconnected Microgrid System,” *IET Renewable Power Generation*, vol. 14, no. 6, pp. 1074-1086, 2020. [CrossRef] [Google Scholar] [Publisher Link]

[9] Shervin Mizani, and Amirnaser Yazdani, “Optimal Design and Operation of a Grid-Connected Microgrid,” *IEEE Electrical Power & Energy Conference*, pp. 1-6, 2009. [CrossRef] [Google Scholar] [Publisher Link]

[10] Amar Kumar Barik, and Dulal Chandra Das, “Proficient Load-Frequency Regulation of Demand Response Supported Bio-Renewable Cogeneration-Based Hybrid Microgrids with Quasi-Oppositional Selfish-Herd Optimization,” *IET Generation, Transmission and Distribution*, vol. 13, no. 13, pp. 2889-2898, 2019. [CrossRef] [Google Scholar] [Publisher Link]

[11] Sarmad Majeed Malik et al., "Cost-Based Droop Scheme for Converters in Interconnected Hybrid Microgrids," *IEEE Access*, vol. 7, pp. 82266-82276, 2019. [CrossRef] [Google Scholar] [Publisher Link]

[12] AvishaTah, and Debapriya Das, "An Enhanced Droop Control Method for Accurate Load Sharing and Voltage Improvement of Isolated and Interconnected DC Microgrids," *IEEE Transactions on Sustainable Energy*, vol. 7, no. 3, pp. 1194-1204, 2016. [CrossRef] [Google Scholar] [Publisher Link]

[13] Jianguo Zhou et al., "Event-Based Distributed Active Power Sharing Control for Interconnected AC and DC Microgrids," *IEEE Transactions on Smart Grid*, vol. 9, no. 6, pp. 6815-6828, 2018. [CrossRef] [Google Scholar] [Publisher Link]

[14] Hao Wang, and Jianwei Huang, "Incentivizing Energy Trading for Interconnected Microgrids," *IEEE Transactions on Smart Grid*, vol. 9, no. 4, pp. 2647-2657, 2018. [CrossRef] [Google Scholar] [Publisher Link]

[15] Chuanlin Zhang et al., "Finite-Time Feedforward Decoupling and Precise Decentralized Control for DC Microgrids towards Large-Signal Stability," *IEEE Transactions on Smart Grid*, vol. 11, no. 1, pp. 391-402, 2020. [CrossRef] [Google Scholar] [Publisher Link]

[16] Mobin Naderi et al., "Interconnected Autonomous AC Microgrids via Back-to-Back Converters—Part I: Small-Signal Modeling," *IEEE Transactions on Power Electronics*, vol. 35, no. 5, pp. 4728-4740, 2020. [CrossRef] [Google Scholar] [Publisher Link]

[17] R. Karthik Kumar, "Fuzzy Tuned PI Controller for Shunt Active Power Filter," *International Journal of Recent Engineering Science*, vol. 7, no. 6, pp. 23-30, 2020. [Google Scholar] [Publisher Link]

[18] C. N. Papadimitriou, V. A. Kleftakis, and N. D. Hatziargyriou, "Control Strategy for Seamless Transition from Islanded to Interconnected Operation Mode of Microgrids," *Journal of Modern Power Systems and Clean Energy*, vol. 5, no. 2, pp. 169-176, 2017. [CrossRef] [Google Scholar] [Publisher Link]

[19] Leong Kit Gan et al., "Limitations in Energy Management Systems: A Case Study for Resilient Interconnected Microgrids," *IEEE Transactions on Smart Grid*, vol. 10, no. 5, pp. 5675-5685, 2019. [CrossRef] [Google Scholar] [Publisher Link]

[20] M. J. Hossain et al., "Robust Control for Power Sharing in Microgrids with Low-Inertia Wind and PV Generators," *IEEE Transactions on Sustainable Energy*, vol. 6, no. 3, pp. 1067-1077, 2015. [CrossRef] [Google Scholar] [Publisher Link]

[21] Isdore Onyema Akwukwaegbu et al., "Design of Model Following Control Integrating PID Controller for DC Servomotor-Based Antenna Positioning System," *SSRG International Journal of Electrical and Electronics Engineering*, vol. 10, no. 6, pp. 33-42, 2023. [CrossRef] [Google Scholar] [Publisher Link]

[22] Mahdi Zolfaghari, MehrdadAbedi, and Gevork B. Gharehpetian, "Power Flow Control of Interconnected AC–DC Microgrids in Grid-Connected Hybrid Microgrids using Modified UIPC," *IEEE Transactions on Smart Grid*, vol. 10, no. 6, pp. 6298-6307, 2019. [CrossRef] [Google Scholar] [Publisher Link]

[23] Hualei Zou et al., "A Survey of Energy Management in Interconnected Multi-Microgrids," *IEEE Access*, vol. 7, pp. 72158-72169, 2019. [CrossRef] [Google Scholar] [Publisher Link]

[24] Farzam Nejabatkhah, and Yun Wei Li, "Overview of Power Management Strategies of Hybrid AC/DC Microgrid," *IEEE Transactions on Power Electronics*, vol. 30, no. 12, pp. 7072-7089, 2015. [CrossRef] [Google Scholar] [Publisher Link]

[25] M. G. Manjula, and S. Surendra, "Integration of Multi-Terminal Unified Power Quality Conditioner in Microgrid System," *International Journal of Recent Engineering Science*, vol. 10, no. 4, pp. 7-13, 2023. [CrossRef] [Google Scholar] [Publisher Link]

[26] C. A. Hans et al., "Hierarchical Distributed Model Predictive Control of Interconnected Microgrids," *IEEE Transactions on Sustainable Energy*, vol. 10, no. 1, pp. 407-416, 2019. [CrossRef] [Google Scholar] [Publisher Link]

[27] H. S. V. S. Kumar Nunna et al., "Multiagent-Based Energy Trading Platform for Energy Storage Systems in Distribution Systems with Interconnected Microgrids," *IEEE Transactions on Industry Applications*, vol. 56, no. 3, pp. 3207-3217, 2020. [CrossRef] [Google Scholar] [Publisher Link]

[28] G.Shabib, Mesalam Abdel Gayed, and A. M. Rashwan, "Optimal Tuning of PID Controller for AVR System using Modified Particle Swarm Optimization," *Proceedings of the 14th International Middle East Power Systems Conference*, Cairo University, Egypt, pp. 305-310, 2010. [Google Scholar] [Publisher Link]

[29] Fangyuan Li et al., "Decentralized Cooperative Optimal Power Flow of Multiple Interconnected Microgrids via Negotiation," *IEEE Transactions on Smart Grid*, vol. 11, no. 5, pp. 3827-3836, 2020. [CrossRef] [Google Scholar] [Publisher Link]

[30] Mohammad Fathi, and Hassan Bevrani, "Statistical Cooperative Power Dispatching in Interconnected Microgrids," *IEEE Transactions on Sustainable Energy*, vol. 4, no. 3, pp. 586-593, 2013. [CrossRef] [Google Scholar] [Publisher Link]

[31] Leong Kit Gan et al., "Data-Driven Energy Management System with Gaussian Process Forecasting and MPC for Interconnected Microgrids," *IEEE Transactions on Sustainable Energy*, vol. 12, no. 1, pp. 695-704, 2021. [CrossRef] [Google Scholar] [Publisher Link]